PHYSICAL REVIEW E **96**, 042138 (2017)

Phase transitions in systems with aggregation and shattering

P. L. Krapivsky,[1] W. Otieno,[2] and N. V. Brilliantov[2]
[1]*Department of Physics, Boston University, Boston, Massachusetts 02215, USA*
[2]*Department of Mathematics, University of Leicester, Leicester LE1 7RH, United Kingdom*
(Received 23 August 2017; published 17 October 2017)

We consider a system of clusters made of elementary building blocks, monomers, and evolving via collisions between diffusing monomers and immobile composite clusters. In our model, the cluster-monomer collision can lead to the attachment of the monomer to the cluster (addition process) or to the total breakup of the cluster (shattering process). A phase transition, separating qualitatively different behaviors, occurs when the probability of shattering events exceeds a certain threshold. The novel feature of the phase transition is the dramatic dependence on the initial conditions.

DOI: 10.1103/PhysRevE.96.042138

I. INTRODUCTION

Addition is the basic growth mechanism generating objects of potentially unlimited size. In the simplest implementation, the process begins with a vast number of identical elementary building blocks, monomers, and larger objects are formed by adding monomers. The smallest composite objects, dimers, arise via the reaction process $M + M \to I_2$, where $M = I_1$ denotes a monomer. A trimer is formed by adding a monomer to a dimer, $M + I_2 \to I_3$, and generally

$$M + I_k \xrightarrow{A_k} I_{k+1}. \tag{1}$$

We tacitly assume that each cluster is fully described by a single parameter, its mass k, which is the number of constituent monomers; the addition process (1) is then characterized by the collection of addition rates A_k.

The addition process (1) mimics aggregating systems in which monomers are mobile, while composite objects (clusters) are immovable. In contrast to the classical aggregation kinetics where all clusters react with each other [1–3], clusters do not directly interact in the process (1). They gradually grow by the addition of monomers. The model (1) has been used to mimic numerous processes such as aggregation of movable monomers and immovable clusters with or without sources [4–6], nonepitaxial growth of thin films [5], formation of colloids [7], instantaneous gelation [8], synthesis of colloids and nanocrystals [9], growth of crystalline nickel particles [10], and kinetics of prion growth [11]. Addition processes also underlie self-assembly (see [12–16]). One important application of this model is to surface science where the monomers are adatoms hopping on the substrate (see, e.g., [17–24]). When two adatoms meet, they form an *immobile* island, a dimer; similarly when an adatom meets an island I_k, it attaches irreversibly forming an island I_{k+1} of mass $k + 1$.

The growth via addition is often counterbalanced by fragmentation of clusters. One possible mechanism is spontaneous evaporation of monomers from islands (see [5,6,17,25–27] and references therein). Another mechanism involves monomer-island collisions. Such collisions may lead to the break of bonds between adatoms comprising the island. Here, we investigate the extreme version positing that islands undergo a total breakup (shattering) into constituting monomers [28,29]:

$$M + I_k \xrightarrow{S_k} \underbrace{M + \cdots + M}_{k+1}, \tag{2}$$

where $k \geqslant 2$ and S_k are the shattering rates; the shattering rates S_k are of course defined only for $k \geqslant 2$. The complete shattering process (2) is rather generic, e.g., in models with strong dominance of small debris with respect to the large ones the emerging cluster distribution is rather similar to the one found in the case of the complete shattering process (see [28]), which follows from the mathematical structure of the according equations.[1]

We ignore spontaneous evaporation of monomers from the islands and investigate the model involving addition (1) and complete shattering (2). We shall show that the interplay between addition and shattering generically results in a phase transition. More precisely, the stationary concentrations of clusters undergo a discontinuous jump when shattering rates exceed some threshold. In particular, if the shattering events are rare, the stationary concentration of monomers vanishes while it becomes finite above the critical shattering rate. This critical rate demarcates qualitatively different states of the system: For the supercritical shattering, the system reaches an equilibrium stationary state independent on the initial conditions. For the subcritical shattering, the stationary states are jammed, that is, they are determined by the initial conditions. Surprisingly, the critical shattering depends on the initial conditions of the system itself.

II. ADDITION AND SHATTERING WITH MASS-INDEPENDENT RATES

For arbitrary addition and shattering rates A_k and S_k, the governing evolution equations read

$$\frac{dc_1}{dt} = -2A_1c_1^2 - c_1\sum_{j\geqslant 2} A_jc_j + c_1\sum_{j\geqslant 2} jS_jc_j, \tag{3a}$$

$$\frac{dc_k}{dt} = c_1A_{k-1}c_{k-1} - c_1(A_k + S_k)c_k. \tag{3b}$$

[1]Although the addition aggregation model differs from that of Ref. [28], similar mathematical reasonings lead to the same conclusion: The emerging cluster distribution C_k for $k \gg 1$ for complete shattering is rather close to the one, if clusters break with a strong domination of small debris.

We start with the simplest model in which the rates of addition and shattering are both mass independent:

$$A_k = 1, \quad S_k = \lambda. \tag{4}$$

One of the mass-independent rates can be set to unity by properly choosing time units, so we have chosen $A_k = 1$.

In the context of surface science, the mass-independent addition rate is particularly natural in the realm of the point-island model (where each island occupies a single lattice site) and in the most interesting case of two-dimensional substrate it provides a good approximation in more realistic cases [17–20,22].

The evolution equations for the model with rates (4) read

$$\frac{dc_1}{dt} = -c_1^2 - c_1 \sum_{j\geqslant 1} c_j + \lambda c_1 \sum_{j\geqslant 2} j c_j, \tag{5a}$$

$$\frac{dc_k}{dt} = c_1 c_{k-1} - c_1 c_k - \lambda c_1 c_k, \quad k \geqslant 2. \tag{5b}$$

Here, c_k is the density of clusters of mass k, so $k = 1$ corresponds to mobile adatoms and $k \geqslant 2$ describe immobile islands. These equations are the straightforward generalization of the addition model [4] where $\lambda = 0$. The first and second terms in the right-hand side of Eq. (5a) give the rate of monomers loss due to aggregation while the third term quantifies the gain of monomers in the shattering events (2) with $S_k = \lambda$. Similarly, the three terms in the right-hand side of Eq. (5b) describe, respectively, the gain of k-mers in the reactions of monomers with the $(k-1)$-mers and loss of the k-mers in the aggregation and shattering processes.

Using (5a) and (5b), one can verify that the mass density $\sum_{j\geqslant 1} j c_j$ remains constant throughout the evolution. We set the mass density to unity (if not stated otherwise)

$$M = \sum_{j\geqslant 1} j c_j = 1. \tag{6}$$

The right-hand side of Eqs. (5a) and (5b) are quadratic polynomials and hence the rate equations are invariant under the transformation $t \to t/M$ and $c_k \to M c_k$. With this transformation, one can set the mass density to unity.

Introducing the auxiliary time

$$\tau = \int_0^t dt'\, c_1(t') \tag{7}$$

we linearize the above equations

$$\frac{dc_1}{d\tau} = \lambda - (1+\lambda)c_1 - N, \qquad N = \sum_{j\geqslant 1} c_j \tag{8a}$$

$$\frac{dc_k}{d\tau} = c_{k-1} - (1+\lambda)c_k, \qquad k \geqslant 2 \tag{8b}$$

$$\frac{dN}{d\tau} = \lambda - (1+\lambda)N. \tag{8c}$$

We used the relation $\sum_{j\geqslant 2} j c_j = 1 - c_1$ which follows from (6) and displayed the rate equation for the total cluster density $N(\tau)$ obtained by summing (8a) and Eqs. (8b) for all $k \geqslant 2$.

We shall always use the monodisperse initial condition

$$c_k(0) = \delta_{k,1} \tag{9}$$

if not stated otherwise. Solving (8c) subject to $N(0) = 1$ gives

$$N(\tau) = \frac{\lambda + e^{-(1+\lambda)\tau}}{1+\lambda}. \tag{10}$$

Plugging (10) into (8a) we obtain a close equation for the density of monomers which is solved to yield

$$c_1 = \left[1 - \frac{\tau}{1+\lambda}\right] e^{-(1+\lambda)\tau} + \frac{\lambda^2}{(1+\lambda)^2}\left[1 - e^{-(1+\lambda)\tau}\right]. \tag{11}$$

To find the evolution of the island densities, we apply to Eqs. (8b) the Laplace transform $\widehat{c}_k = \int_0^\infty c_k(\tau) e^{-p\tau} d\tau$. Since $c_k(0) = 0$ for $k \geqslant 2$, we obtain

$$p\widehat{c}_k = \widehat{c}_{k-1} - (1+\lambda)\widehat{c}_k, \qquad k \geqslant 2 \tag{12}$$

from which

$$\widehat{c}_k(p) = \frac{\widehat{c}_1(p)}{(p+1+\lambda)^{k-1}}, \qquad k \geqslant 2. \tag{13}$$

It is straightforward to find the Laplace transform of $c_1(\tau)$ given by (11); substituting the result into Eq. (13) and performing the inverse Laplace transform, we obtain

$$c_{k+1}(\tau) = \frac{\tau^k}{\Lambda k!}\left[\frac{2\Lambda - 1}{\Lambda} - \frac{\tau}{k+1}\right] e^{-\Lambda\tau} + \frac{(\Lambda-1)^2 \gamma(k, \Lambda\tau)}{\Lambda^{k+2}(k-1)!}, \tag{14}$$

where

$$\gamma(k,a) = \int_0^a du\, u^{k-1} e^{-u} \tag{15}$$

is the incomplete gamma function. Hereinafter, we often shortly write $\Lambda \equiv \lambda + 1$. If $\tau \to \infty$ as $t \to \infty$, the final cluster density and the final total density are

$$C_k \equiv c_k(\tau = \infty) = \frac{\lambda^2}{(1+\lambda)^{k+1}}, \quad k \geqslant 1 \tag{16}$$

$$N(\tau = \infty) = \frac{\lambda}{1+\lambda}. \tag{17}$$

Exactly the same result is obtained if one seeks the stationary solution to Eqs. (8a)–(8c).

Naively, one would expect that the system evolves to the equilibrium state (16) and (17) independently on initial conditions. The actual behavior is richer, namely, the densities may relax to a state dramatically different from the equilibrium solution (16) and (17) (see Fig. 1).

To understand this surprising behavior, we notice that the monomer density given by (11) is physically applicable as long as $c_1 \geqslant 0$. For sufficiently large shattering rates the monomer density is always positive, while for smaller rates $c_1(\tau)$ first vanishes at a certain $\tau_{\max}(\lambda)$. In these situations, the physical range $0 \leqslant t < \infty$ corresponds to $0 \leqslant \tau < \tau_{\max}(\lambda)$, so that the above assumption that $t \to \infty$ as $\tau \to \infty$ is not valid. More precisely, $\tau_{\max}(\lambda)$ is finite when $\lambda \leqslant \lambda_c$, while for $\lambda > \lambda_c$ the monomer density remains positive for all $0 < \tau < \infty$. This is obvious from Fig. 2. To establish this assertion analytically, we first notice that $c_1(\tau)$ given by (11) reaches minimum when

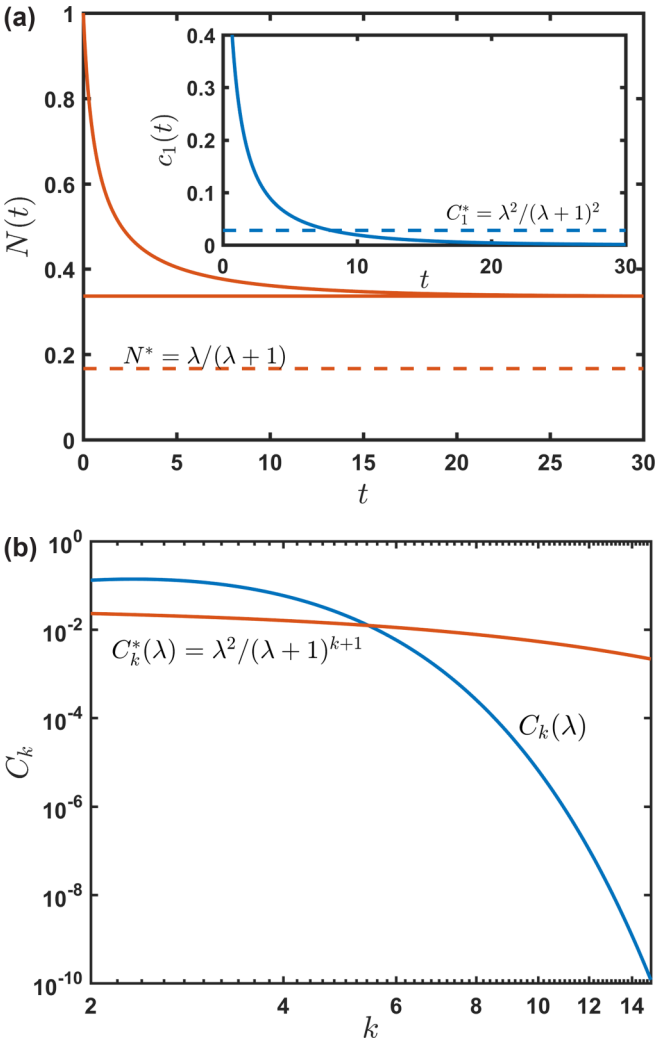

FIG. 1. (a) Evolution of the monomer density $c_1(t)$ and total cluster density $N(t)$ for the case of constant kernels and the monodisperse initial condition when $\lambda = 0.2$. The system approaches a final state $c_1(t=\infty)$ and $N(t=\infty)$ which differs from the equilibrium state (16) and (17). (b) Asymptotic cluster size distribution $c_k(t=\infty)$ dramatically differs from the equilibrium distribution (16).

$\tau = 2$, from which the minimal possible value is

$$c_1^{\min} = \left[1 - \frac{2}{1+\lambda}\right] e^{-2(1+\lambda)} + \frac{\lambda^2}{(1+\lambda)^2}[1 - e^{-2(1+\lambda)}].$$

Analyzing this expression we find that it remains positive when $\lambda > \lambda_c$ where λ_c is the root of $e^{1+\lambda_c} = 1/\lambda_c$, that is, $\lambda_c = W(1/e)$, where $W(x)$ is the Lambert function; numerically $\lambda_c = 0.278\,46\ldots$.

Different behaviors emerge depending on whether λ is smaller, equal, or larger than λ_c.

A. Subcritical regime: $\lambda < \lambda_c$

In the region $0 \leqslant \lambda < \lambda_c$ the monomer density vanishes at a certain $\tau_{\max}(\lambda)$ which is found from (11) to be the root of the transcendental equation

$$e^{(1+\lambda)\tau_{\max}} = \frac{(1+\lambda)\tau_{\max} - 1 - 2\lambda}{\lambda^2}. \tag{18}$$

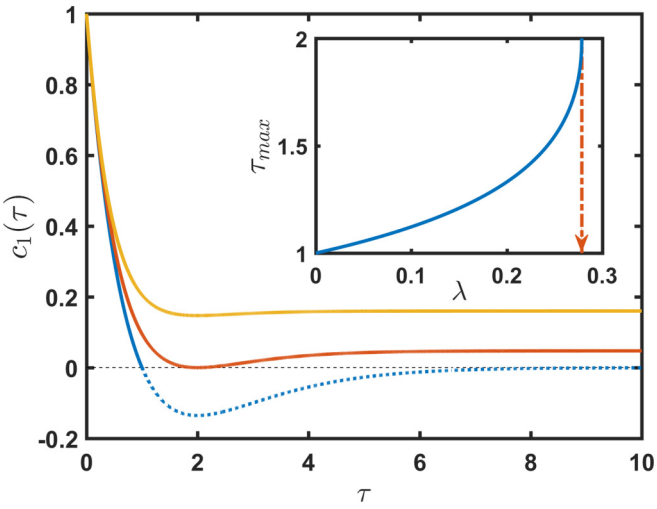

FIG. 2. The monomer density $c_1(\tau)$ remains positive when the shattering rate satisfies $\lambda > \lambda_c \approx 0.278\,46$. Shown (bottom to top) is the monomer density for $\lambda = 0, \lambda_c, 2/3$. Inset: when physical time diverges, $t \to \infty$, the auxiliary time for $\lambda < \lambda_c$, remains finite, $\tau \to \tau_{\max}(\lambda)$.

The solution of Eq. (18) may be expressed in terms of the Lambert function

$$\tau_{\max} = \frac{1 + 2\lambda - W(-\lambda^2 e^{2\lambda+1})}{1+\lambda}. \tag{19}$$

Note that $\tau_{\max}$ increases from 1 to 2 as λ increases from 0 to λ_c (see Fig. 2). For $\tau_{\max} = 1$ and $\lambda = 0$, Eq. (14) reproduces the final distribution of cluster sizes for the additional aggregation without shattering [4].

The monomer density vanishes exponentially in terms of the physical time

$$c_1 \sim e^{-t(N_\infty - \lambda)}, \qquad t \to \infty$$

and the island densities saturate at $t \to \infty$, that is, $C_k(\lambda) \equiv c_k(\tau_{\max}) > 0$ for $k \geqslant 2$, with $c_k(\tau)$ and $\tau_{\max}$ given, respectively, by Eqs. (14) and (19); the same is true for the final density of islands $N_\infty(\lambda) = N[\tau_{\max}(\lambda)]$ which is positive for all $\lambda \geqslant 0$.

Analyzing (10) and (18), one finds that in the subcritical region $N_\infty(\lambda)$ is a decreasing function of the shattering rate λ, namely, it decreases from $N_\infty(0) = e^{-1} \approx 0.367\,88$ to $N_\infty(\lambda_c) = \lambda_c$ (see Fig. 3). The approach of $N_\infty(\lambda)$ to the density $N_\infty(\lambda_c) = \lambda_c$ in the critical regime is singular:

$$N_\infty(\lambda) - N_\infty(\lambda_c) \simeq 2\lambda_c \sqrt{\frac{\lambda_c}{1+\lambda_c}} \sqrt{\lambda_c - \lambda} \tag{20}$$

as $\lambda \uparrow \lambda_c$.

B. Critical regime: $\lambda = \lambda_c$

In the critical regime the monomer density (11) also vanishes. More precisely, when $\tau \to \tau_{\max}(\lambda_c) = 2$, the monomer density decreases as $c_1 \simeq \frac{1}{2}\lambda_c^2 (2-\tau)^2$ which can be rewritten as

$$c_1(t) \simeq \frac{2}{\lambda_c^2} \frac{1}{t^2} \tag{21}$$

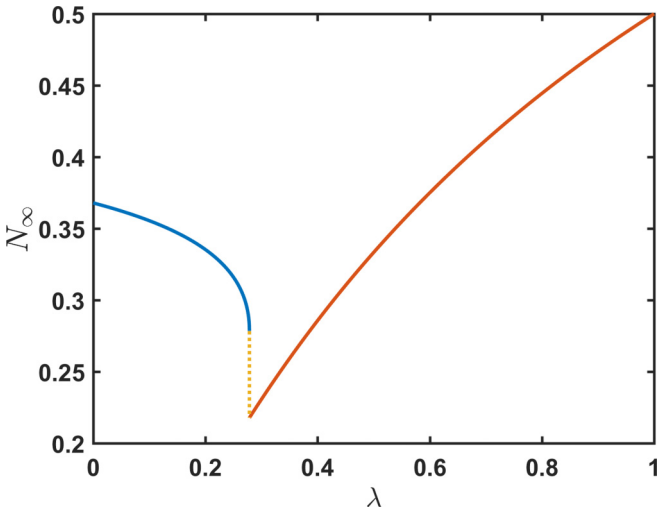

FIG. 3. The final density of clusters $N_\infty(\lambda)$ is a decreasing function of λ in the range $0 \leqslant \lambda \leqslant \lambda_c \approx 0.278\,46$; it undergoes a first order transition at λ_c, and becomes an increasing function of λ in the range $\lambda > \lambda_c$ where $N_\infty = N^* = \lambda/(1+\lambda)$.

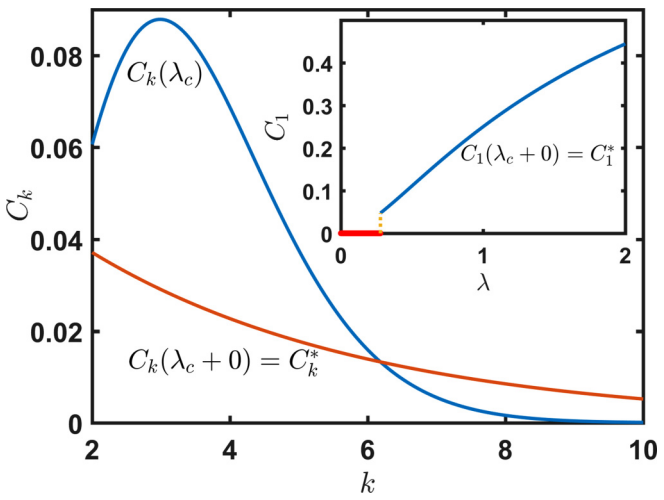

FIG. 4. The discontinuous jump in the cluster size distribution from $C_k(\lambda_c)$ to $C_k(\lambda_c + 0)$, given by Eq. (16) at the critical point $\lambda = \lambda_c$. Inset: the final density of monomers $C_1(\lambda)$ vanishes in the range $0 \leqslant \lambda \leqslant \lambda_c \approx 0.278\,465$, undergoes a first order transition at λ_c, and becomes an increasing function of λ in the supercritical region $\lambda > \lambda_c$ where $C_1 = \lambda^2/(1+\lambda)^2$.

in terms of the original time variable. Thus, in the critical regime the process slows down: the vanishing is algebraic rather than exponential.

The total density of clusters also exhibits an algebraic approach to the final density:

$$N(t) - N_\infty \simeq \frac{2}{t}, \tag{22}$$

where $N_\infty = N_\infty(\lambda_c) = \lambda_c$. The asymptotic (22) follows from (10). The decay exponent in (22) is twice smaller than the exponent characterizing the decay of monomers.

The approach to the final density for any species of islands is similar to (22), viz.,

$$c_k(t) - C_k \simeq \frac{B_k}{t}. \tag{23}$$

Using (5b) one can express the amplitudes B_k through the final densities $C_k \equiv c_k(\tau = 2)$:

$$B_k = 2\,\frac{\Lambda_c C_k - C_{k-1}}{(\Lambda_c - 1)^2}, \qquad \Lambda_c = 1 + \lambda_c \tag{24}$$

for $k \geqslant 2$. The final densities can be expressed using Eq. (14) with $\tau_{\max} = 2$. One finds

$$\frac{C_{k+1}}{(\Lambda_c - 1)^2} = \frac{2^k}{\Lambda_c k!}\left[\frac{2\Lambda_c - 1}{\Lambda_c} - \frac{2}{k+1}\right] + \frac{\gamma(k, 2\Lambda_c)}{\Lambda_c^{k+2}(k-1)!}. \tag{25}$$

Combining (25) with (24) we get

$$B_k = -2^{k-1}\,\frac{(k-1)(k-4)}{k!}, \tag{26}$$

where we have used the identity

$$(k-1)\gamma(k-1, 2\Lambda) - \gamma(k, 2\Lambda) = (2\Lambda)^{k-1} e^{-2\Lambda} \tag{27}$$

which can be derived by substituting the definition (15) into (27) and performing the integration by part of the second integral on the left-hand side. We also use the identity $e^{-\Lambda_c} = \Lambda_c - 1$ obeyed by $\Lambda_c = 1 + \lambda_c$. Remarkably, the amplitudes B_k are independent on Λ_c and rational.

C. Supercritical region: $\lambda > \lambda_c$

In the supercritical case $\tau \to \infty$ as $t \to \infty$ and we can use Eq. (16) for the final cluster densities $C_k(\lambda)$:

$$C_k(\lambda) = \frac{\lambda^2}{(1+\lambda)^{k+1}} = C_k^*, \qquad k \geqslant 1. \tag{28}$$

Thus, the final monomer density exhibits a discontinuous (first order) phase transition as a function of λ:

$$C_1(\lambda) = \begin{cases} 0, & \lambda \leqslant \lambda_c \\ \frac{\lambda^2}{(1+\lambda)^2}, & \lambda > \lambda_c \end{cases} \tag{29}$$

(see Fig. 4). The total cluster density also exhibits the discontinuous phase transition at $\lambda = \lambda_c$, more precisely

$$N_\infty(\lambda) = \begin{cases} \lambda_c, & \lambda = \lambda_c \\ \frac{\lambda_c}{1+\lambda_c}, & \lambda = \lambda_c + 0. \end{cases} \tag{30}$$

The same is valid for the final densities C_k which undergo a jump at the critical point $\lambda = \lambda_c$ from the values $C_k(\lambda_c)$, given by Eq. (25), to $C_k(\lambda_c + 0) = \lambda_c^2/(1+\lambda_c)^{k+1}$, as it is illustrated in Fig. 4.

D. Dependence on initial conditions

The previous analysis has been done for the monodisperse initial condition (9). We now briefly discuss more general initial conditions. (We still set $M = 1$.) The behavior in the supercritical region is universal, e.g., the final densities given by (28) do not depend on the initial condition. The critical shattering rate is not universal, however, namely it depends on the initial condition. As an example, consider the initial condition

$$c_1(0) = c_2(0) = 1/3\,, \quad c_k(0) = 0 \quad \text{when} \quad k \geqslant 3, \tag{31}$$

which corresponds to $N(0) = \frac{2}{3}$. Performing the same steps that led to Eq. (11), we obtain the monomer density for the above initial conditions:

$$c_1 = \frac{1}{3}\left[1 - \frac{2-\lambda}{1+\lambda}\tau\right]e^{-(1+\lambda)\tau} + \frac{\lambda^2}{(1+\lambda)^2}[1 - e^{-(1+\lambda)\tau}].$$

The qualitative behaviors remain the same. Chief quantitative results are also universal, e.g., in the critical regime the monomer density exhibits the t^{-2} decay. The critical shattering rate is, however, $\lambda_c \approx 0.300\,57$ for the initial condition (31).

For an arbitrary initial condition solution of Eqs. (8a) and (8c) yield for the total cluster and monomer density

$$N(\tau) = \frac{\lambda}{1+\lambda}[1 - e^{-(1+\lambda)\tau}] + N_0\, e^{-(1+\lambda)\tau}, \tag{32}$$

$$c_1(\tau) = c_{1,0}\, e^{-(1+\lambda)\tau} - \left[N_0 - \frac{\lambda}{1+\lambda}\right]\tau\, e^{-(1+\lambda)\tau} + \frac{\lambda^2}{(1+\lambda)^2}[1 - e^{-(1+\lambda)\tau}], \tag{33}$$

where $N_0 = N(0)$ and $c_{1,0} = c_1(0)$. Preforming again the Laplace transform and using the Laplace transform of $c_1(\tau)$ given by (33), we find the cluster size distribution for arbitrary initial conditions:

$$c_{k+1}(\tau) = \frac{\tau^k}{k!}\left[c_{1,0} - C_1^* - (N_0 - N^*)\frac{\tau}{k+1}\right]e^{-\Lambda\tau} + \frac{(\Lambda-1)^2\gamma(k,\Lambda\tau)}{\Lambda^{k+2}(k-1)!} + c_{k,0}\, e^{-\Lambda\tau}. \tag{34}$$

Here, $c_{k,0} = c_k(0)$ and we use the shorthand notations $N^* \equiv \lambda/(1+\lambda)$ for the equilibrium cluster density and $C_1^* \equiv \lambda^2/(1+\lambda)^2$ for the equilibrium density of monomers.

There are again three regimes. In the supercritical regime, $c_1(\tau) > 0$ for all τ. In this case, $\tau \to \infty$ as $t \to \infty$ and the final distribution (28) of cluster sizes C_k is universal and independent on the initial conditions. In the subcritical regime, $c_1(\tau) \geqslant 0$ for $\tau \leqslant \tau_{\max}$ and $c_1(\tau) < 0$ otherwise. In the critical regime, $c_1(\tau) \geqslant 0$ for all τ and $c_1(\tau_{\max}) = 0$. For the critical and subcritical regimes, $\tau \to \tau_{\max} < \infty$ as $t \to \infty$ and the distribution C_k is not universal, namely, it depends on the initial conditions.

We emphasize that two parameters N_0 and $c_{1,0}$ play the crucial role in the critical and subcritical regimes as they demarcate the emergence of these regimes and determine the final modified time $\tau_{\max}$. Using (33) one can find the domain in the $(N_0, c_{1,0})$ phase plane where $c_1(\tau) > 0$ for all τ[2]

$$\frac{(1+\lambda)c_{1,0} + N_0 - \lambda}{N_0 - N^*} > \ln\left(\frac{N_0 - N^*}{\lambda N^*}\right). \tag{35}$$

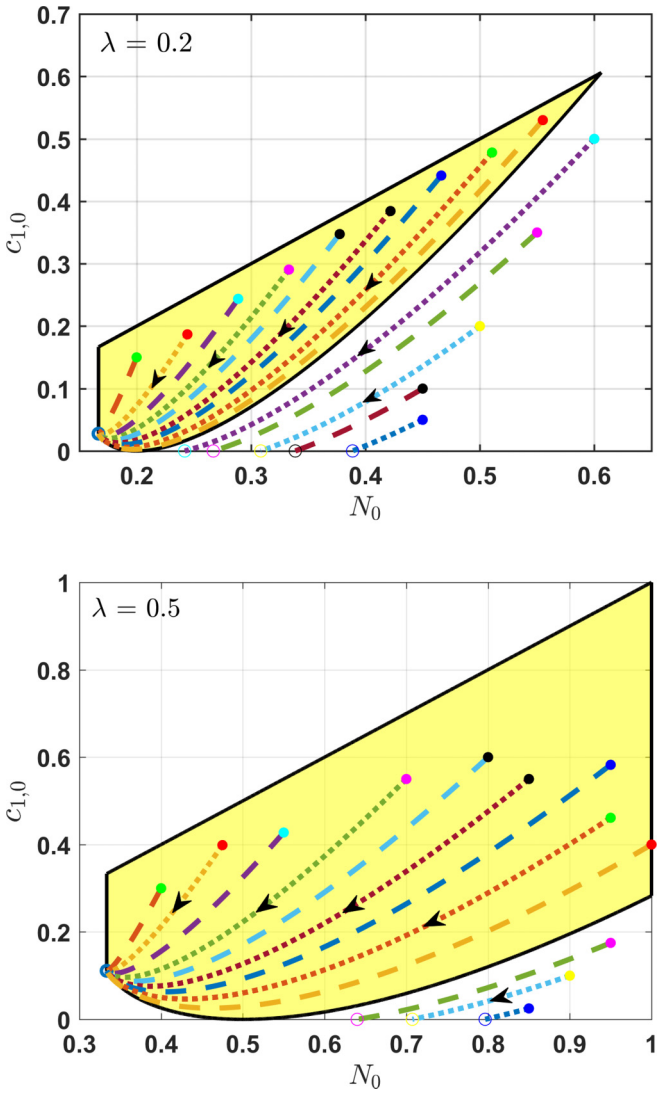

FIG. 5. Phase trajectories for the total density $N(t)$ and the density of monomers $c_1(t)$ for different initial conditions. The region marked by yellow corresponds to the supercritical regime, where all trajectories terminate at the universal point, $N^* = \lambda/(1+\lambda)$, $C_1^* = \lambda^2/(1+\lambda)^2$. The curved part of the boundary of the yellow domain corresponds to the critical regime. For the initial conditions, located outside the yellow domain (and satisfying $c_{1,0} \leqslant N_0$) the subcritical regime is realized; the trajectories terminate in this case on the axis $c_1 = 0$.

[2]This may be done in the same manner as for the case of monodisperse initial conditions: First, we find $\tau_{\max}$ from the condition $dc_1(\tau)/d\tau = 0$ at $\tau = \tau_{\max}$, then $c_1(\tau_{\max}) > 0$ may be recast into the form of Eq. (35).

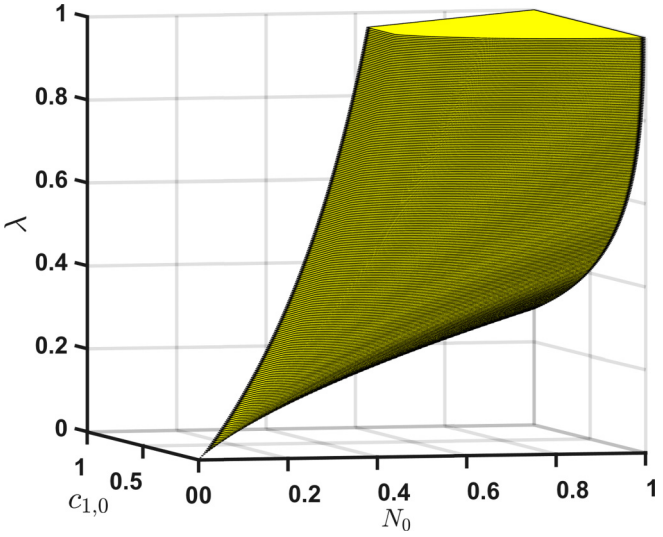

FIG. 6. The 3D plot of the critical shattering λ_c as the function of the initial conditions N_0, $c_{1,0}$ for the model with constant kinetic rates (4). The domain inside the depicted surface corresponds to the supercritical behavior of the system; Fig. 5 provides the cross sections of this surface for particular values of λ.

(Needless to say, $c_{1,0} \leqslant N_0$ should be also obeyed.) Within this domain, all trajectories in the (N,c_1) plane terminate at the universal point (N^*, C_1^*). If Eq. (35) turns into equality, it determines the critical shattering rate λ_c, thereby yielding the dependence on the initial conditions: $\lambda_c = \lambda_c(N_0,c_{1,0})$.

Outside of the domain given by (35), the trajectories terminate on the axis $c_1 = 0$ with N_∞ depending on the initial conditions. This is illustrated in Fig. 5.

Figure 6 shows the dependence of the critical shattering λ_c on the initial conditions N_0 and $c_{1,0}$. As it may be seen from Fig. 6, the larger λ_c the larger the domain of the initial conditions corresponding to the supercritical regime, where the system eventually arrives at the universal steady state.

III. ADDITION AND SHATTERING WITH ARBITRARY RATES

In the previous section, we studied the addition and shattering processes with mass-independent rates (4). A more general class of models is characterized by rates which vary algebraically: $A_k = k^a$ and $S_k = \lambda k^s$. In this section, we limit ourselves for the case of $a = s$. We start with $a = s = 1$, which admits some analytical treatment.

A. Kinetic rates proportional to the cluster mass

For the model with linear rates, $A_k = k$ and $S_k = \lambda k$, the kinetic equations read

$$\frac{dc_1}{d\tau} = -(1+\lambda)c_1 - 1 + \lambda M_2, \tag{36a}$$

$$\frac{dc_k}{d\tau} = (k-1)c_{k-1} - (1+\lambda)kc_k, \quad k \geqslant 2. \tag{36b}$$

The second moment $M_2 = \sum_{k\geqslant 1} k^2 c_k$ of the cluster size distribution appears in (36a). Generally the αth moment is defined by $M_\alpha = \sum_{k\geqslant 1} k^\alpha c_k$.

To determine the monomer density, one needs to know M_2. The rate equation for the second moment is simple,

$$\frac{dM_2}{d\tau} = 2M_2 + \lambda(M_2 - M_3), \tag{37}$$

yet it involves the third moment. The rate equation for the third moment similarly involves the fourth moment. This continues ad infinitum leading to (seemingly) unsolvable hierarchy.

1. Supercritical regime

For the supercritical region $\lambda > \lambda_c$ we easily find the equilibrium densities. Indeed, Eq. (36b) turns into the simple recurrence $(1+\lambda)kC_k = (k-1)C_{k-1}$, from which one gets the equilibrium cluster size distribution

$$C_k = \frac{C_1}{k(1+\lambda)^{k-1}}.$$

Using the condition for the mass density $\sum_{k\geqslant 1} kC_k = 1$, we fix $C_1 = \lambda/(1+\lambda)$, which yields

$$C_k = \frac{\lambda}{(1+\lambda)^k}\,\frac{1}{k} = C_k^*. \tag{38}$$

2. Subcritical and critical regimes

First, we consider the monodisperse initial condition. Applying again the Laplace transform to (36b) yields

$$p\widehat{c}_k = (k-1)\widehat{c}_{k-1} - (1+\lambda)k\widehat{c}_k, \quad k \geqslant 2. \tag{39}$$

Solving this recurrence we express all $\widehat{c}_k(p)$ through $\widehat{c}_1(p)$:

$$\widehat{c}_k(p) = \frac{\widehat{c}_1(p)}{(1+\lambda)^{k-1}}\,\frac{\Gamma(k)\Gamma(1+\Pi)}{\Gamma(k+\Pi)} \tag{40}$$

with $\Pi = 1 + (1+\lambda)^{-1}p$. Applying the Laplace transform for the mass conservation (6) we obtain

$$\sum_{k\geqslant 1} k\widehat{c}_k(p) = \frac{1}{p}. \tag{41}$$

Plugging then (40) into (41), we find the Laplace transform of the monomer density:

$$\widehat{c}_1 = p^{-1}\,\frac{1}{F[1,2;1+\Pi;(1+\lambda)^{-1}]}, \tag{42}$$

where $F[a,b;c;z] = \sum_{n\geqslant 0} \frac{(a)_n (b)_n}{(c)_n}\frac{z^n}{n!}$ is the hypergeometric function.

Near the origin, $p \to 0$,[3] we have $\Pi \to 2$, and using identity $F[1,2;2;z] = (1-z)^{-1}$, we find that $\widehat{c}_1$ has a simple pole with residue $\lambda/(1+\lambda)$. This is consistent with the monomer density $c_1(\tau)$ quickly approaching the steady-state value $C_1 = \lambda/(1+\lambda)$ which agrees with (38).

The precise value of the critical shattering amplitude λ_c corresponding to the monodisperse initial condition is hidden in the exact Laplace transform of the monomer density (42),

[3]The condition $p \to 0$ corresponds to $\tau \to \infty$, that is, to the supercritical case.

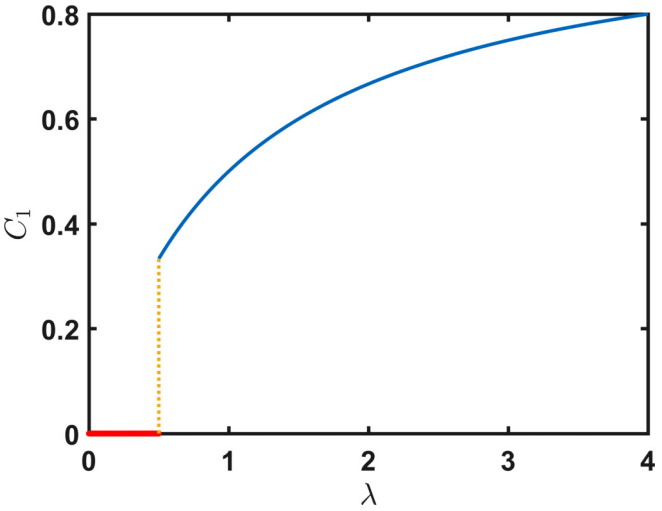

FIG. 7. For the case of linear kernels, $A_k = k$ and $S_k = \lambda k$, the final density of monomers undergoes a first order phase transition at $\lambda = \lambda_c = \frac{1}{2}$ in the situation when initially almost all clusters are dimers. The final density of monomers is given by (44) in this case.

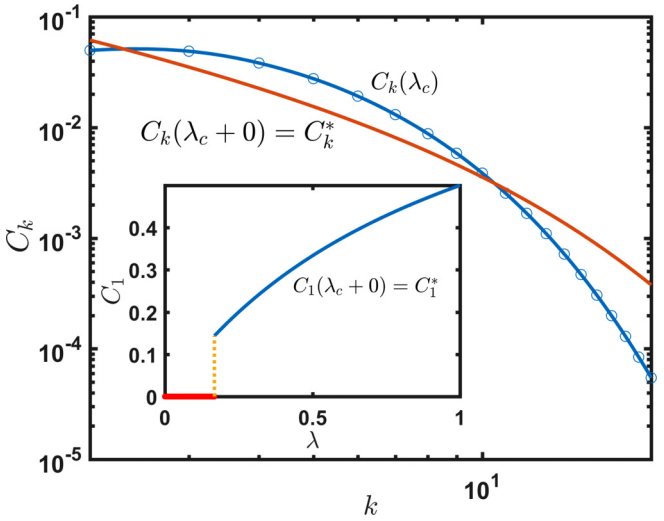

FIG. 8. For the case of the linear kernels, $A_k = k$ and $S_k = \lambda k$, the discontinuous jump in the cluster size distribution from $C_k(\lambda_c)$ to $C_k(\lambda_c + 0)$ [see Eq. (38)] happens for monodisperse initial conditions at the critical point $\lambda_c = 0.167\,732\,77\ldots$. Inset: the final density of monomers $C_1(\lambda)$ vanishes in the range $0 \leqslant \lambda \leqslant \lambda_c$ and undergoes a first order transition at λ_c. In the supercritical region $\lambda > \lambda_c$, C_1 is given by Eq. (38).

but difficult to extract. We now show that $\lambda_c > 0$ at least for some initial conditions.

Let us consider a simple case when initially only monomers and dimers present in the system, so that

$$c_{1,0} = 2N_0 - 1; \quad c_{2,0} = 1 - N_0; \quad M_2(0) = 3 - 2N_0. \tag{43}$$

Equation (36a) becomes

$$\frac{dc_1}{d\tau} = -(1+\lambda)c_1 - 1 + \lambda(3 - 2N_0)$$

when $\tau \ll 1$. Let almost all clusters are dimers, then starting with $c_{1,0} = 2N_0 - 1 \ll 1$, the monomer density quickly crosses zero if

$$\lambda(3 - 2N_0) < 1 + (1+\lambda)(2N_0 - 1),$$

that is, $\lambda < N_0/2(1 - N_0)$. Since $N_0 = c_{1,0} + c_{2,0} \simeq c_{2,0}$ and $M = 1 = c_{1,0} + 2c_{2,0} \simeq 2c_{2,0}$, we conclude that $\lambda_c \to \frac{1}{2}$. Thus, in this case (see also Fig. 7)

$$C_1 = \begin{cases} 0, & \lambda < \frac{1}{2} \\ \frac{\lambda}{1+\lambda}, & \lambda > \frac{1}{2}. \end{cases} \tag{44}$$

For the monodisperse initial conditions, the critical value of λ may be found numerically, $\lambda_c = 0.167\,732\,77\ldots$. The final concentrations of clusters $C_k(\lambda_c)$ and monomers $C_1(\lambda_c)$ also found numerically undergo a first order phase transition to the values $C_k(\lambda_c + 0)$ and monomers $C_1(\lambda_c + 0)$, given by Eq. (38) (see Fig. 8).

The dependence of the evolution regime on the initial conditions is not anymore simple, as in the case of constant kernels, when only the concentration of monomers and the total number of clusters were important. For $A_k = k$ and $S_k = \lambda k$ all initial concentrations $c_k(0)$ are determinative. Figure 9 shows the domain in the space of the initial concentrations of the monomers $c_{1,0}$, dimers $c_{2,0}$, and trimers $c_{3,0}$, corresponding to the supercritical regime, when $c_{4,0} = (1 - c_{1,0} - 2c_{2,0} - 3c_{3,0})/4$ and all other initial concentrations are zero, $c_k(0) = 0$ for $k \geqslant 5$.

B. Kinetic rates $A_k = k^s$ and $S_k = \lambda k^s$

Here, we consider a family of models with proportional algebraic rates: $A_k = k^s$ and $S_k = \lambda k^s$. We consider the range $s \leqslant 1$. This is physically motivated since the reaction rates

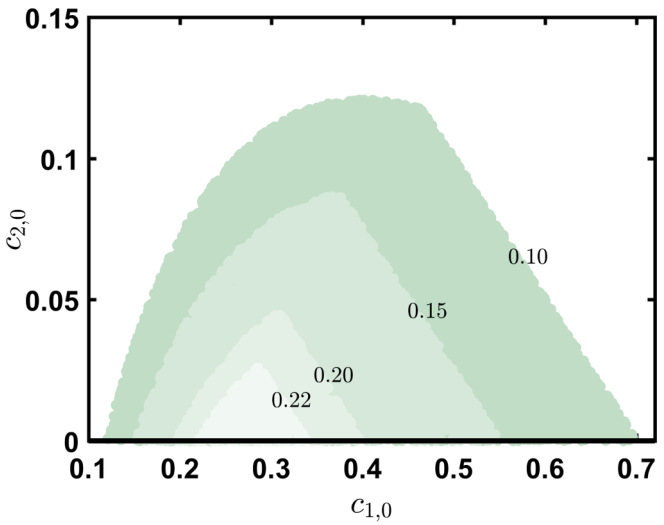

FIG. 9. The boundaries of the supercritical region in the phase plane $(c_{1,0}, c_{2,0})$ for different values of $c_{3,0}$. For each contour, with the value of $c_{3,0}$ indicated on the plot, the supercritical region lies inside the contour. The initial densities $c_{k,0} = 0$ for $k \geqslant 5$ and $c_{4,0} = (1 - c_{1,0} - 2c_{2,0} - 3c_{3,0})/4$ have been chosen. The rate kernels are $A_k = k$, $S_k = \lambda k$, and $\lambda = 0.167\,732\,77\ldots$ (which corresponds to λ_c for the monodisperse initial condition).

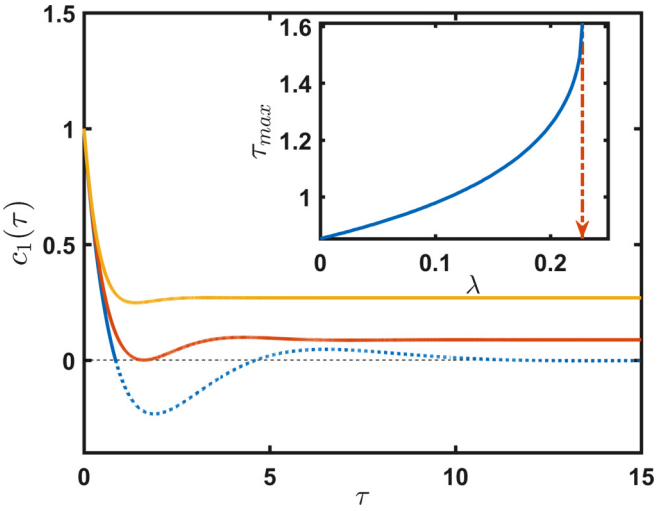

FIG. 10. Evolution of the monomer density $c_1(\tau)$ for supercritical, critical, and subcritical regimes for the monodisperse initial condition. Shown are results for the model with kernels $A_k = \sqrt{k}$ and $S_k = \lambda\sqrt{k}$. The critical shattering rate in this case is $\lambda_c = 0.227\,792\,010\,3\ldots$.

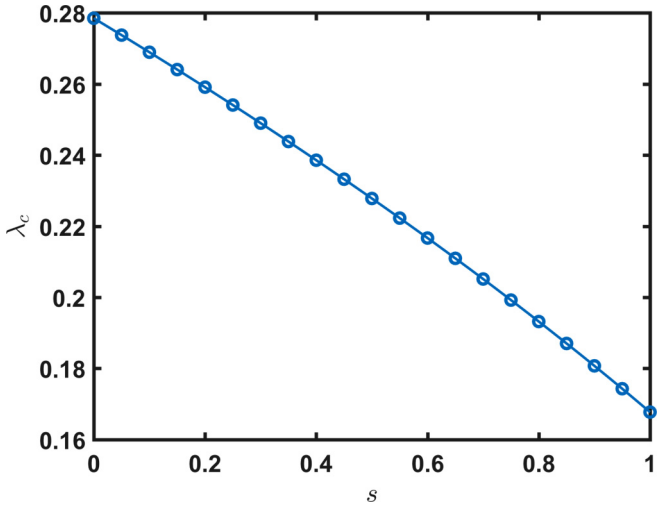

FIG. 11. The dependence of the critical shattering rate λ_c on the exponent s in the case of the monodisperse initial condition. The critical rate λ_c separates the supercritical evolution regime ($\lambda > \lambda_c$) and subcritical regime ($\lambda < \lambda_c$).

cannot increase faster than mass. Moreover, the models with $s > 1$ are mathematically ill defined as instantaneous gelation may occur (it certainly occurs for the pure addition process, see [4,8]).

The rate equations read

$$\frac{dc_1}{d\tau} = -(1+\lambda)c_1 - M_s + \lambda M_{1+s}, \tag{45a}$$

$$\frac{dc_k}{d\tau} = (k-1)^s c_{k-1} - (1+\lambda)k^s c_k, \quad k \geqslant 2. \tag{45b}$$

Equation (45a) contains the moments M_s and M_{1+s} that satisfy

$$\frac{dM_b}{d\tau} = \sum_{k=1}^{\infty}[(k+1)^b - (1+\lambda)k^b]k^s c_k - M_s + \lambda M_{1+s}$$

with $b = s$ and $1+s$. These equations are not closed and for noninteger s they cannot be even written in terms of the moments only.

Equations (45a) and (45b) still admit some analytical treatment in the supercritical regime ($\lambda > \lambda_c$). The equilibrium densities straightforwardly follow from the recursion $k^s(1+\lambda)C_k = (k-1)^s C_{k-1}$ and the mass density $M = 1$. One gets

$$C_k = \frac{1}{k^s \Lambda^k \mathrm{Li}_{s-1}(\Lambda^{-1})}, \tag{46}$$

where $\Lambda = 1 + \lambda$ as before, and $\mathrm{Li}_\nu(x) = \sum_{j\geqslant 1} x^j/j^\nu$ is the polylogarithm function. We have $\mathrm{Li}_0(x) = x/(1-x)$ and thus for $s = 1$ we recover the previous result (38).

Overall, our simulations show the same qualitative behavior as for $s = 0$ and 1. Namely, for any initial condition there exists a supercritical domain with the final densities given by Eq. (46) and $C_1 > 0$. This is illustrated in Fig. 10, where the evolution of monomer density is shown for $s = 0.5$ for supercritical, critical, and subcritical regimes for the case of monodisperse initial conditions.

The critical shattering rate decreases with increasing s (see Fig. 11) on the interval $0 \leqslant s \leqslant 1$. The maximum and minimum values of λ_c are, respectively, $W(1/e) = 0.278\,464\,5\ldots$ for $s = 0$ and $0.167\,732\,8\ldots$ for $s = 1$.

As in the models with $s = 0$ and 1, the final densities of clusters C_k and monomers C_1 undergo a jump at the critical point from $C_k(\lambda_c)$ to the supercritical values $C_k(\lambda_c + 0)$ given by (46). As previously, the final monomer density vanishes for the subcritical and critical cases, i.e., $C_1 = 0$ for $\lambda \leqslant \lambda_c$. The plots for any $0 < s < 1$ look very similar to Figs. 4 and 8.

The dependence of the critical shattering on the initial conditions is again not simple since λ_c depends on all initial concentrations $c_k(0)$, $k \geqslant 1$. Accordingly, the supercritical

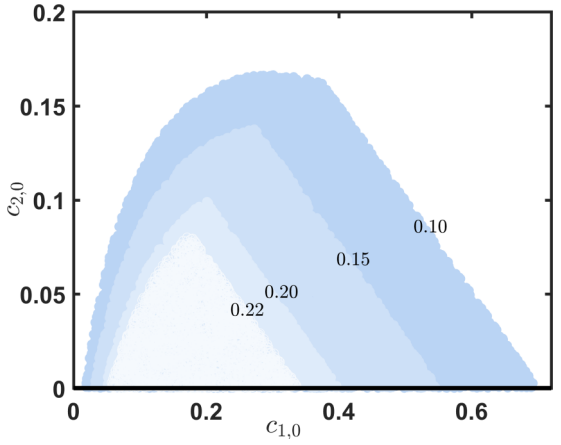

FIG. 12. The boundaries of the supercritical region in the phase plane $(c_{1,0}, c_{2,0})$ for different values of $c_{3,0}$. Shown are results for the model with kernels $A_k = \sqrt{k}$ and $S_k = \lambda\sqrt{k}$ in the case when the initial densities are $c_{k,0} = 0$ for $k \geqslant 5$ and $c_{4,0} = (1 - c_{1,0} - 2c_{2,0} - 3c_{3,0})/4$. The shattering rate is $\lambda = 0.227\,792\,010\,3\ldots$ (it corresponds to λ_c for the monodisperse initial condition).

domain depends for each $\lambda > 0$ on all initial concentrations. This is illustrated in Fig. 12, where the boundaries of the supercritical domain are shown.

IV. CONCLUSION

We investigated a model involving aggregation and fragmentation kinetics where immobile clusters (islands) interact with mobile monomers. The outcome of the monomer-cluster interactions may be twofold: the monomer may attach to the cluster or the cluster may shatter into monomers. This model mimics the growth of islands on a surface in epitaxy processes when a collision of an adatom (monomer) with an island is accompanied by the transmission of the adatom's energy to the island. If the transmitted energy is small, the adatom joins the island; if the energy is large, the island may fragment into adatoms. In a similar Becker-Doering model (see [26] for a review) the decomposition of islands occurs through spontaneous evaporation of monomers. We focus on the decomposition of clusters due to collisions with mobile monomers which could be a dominating decomposition mechanism at least in situations when the energy transmitted in a collision is the major perturbation (e.g., the thermal fluctuations transmitted to a cluster from the substrate are relatively small).

We considered a class of models with addition rates varying algebraically with cluster size: $A_k = k^s$. We assumed that the shattering rate is proportional to the addition rate $S_k = \lambda A_k$, where λ quantifies the shattering intensity. The proportionality of the aggregation and shattering rates has been justified through the computation of the rates in some models [28].

When $s = 0$, the addition and shattering rates are mass independent. This model admits a comprehensive analytical analysis and demonstrates the most prominent features of aggregating and shattering systems. We also analyzed the model with $s = 1$, and studied numerically the models with $0 < s < 1$. All these models are characterized by three different evolution regimes. In the supercritical regime $\lambda > \lambda_c$, the system evolves to a final equilibrium state which is universal, i.e., it does not depend on the initial conditions. For the critical and subcritical regimes, $\lambda \leqslant \lambda_c$, the evolution terminates at a nonequilibrium *jammed* state depending on the initial conditions. In subcritical regimes, $\lambda < \lambda_c$, the evolution to a final jammed state is exponentially fast in time; in the critical regime, $\lambda = \lambda_c$, the evolution is algebraic. The transition from an equilibrium to a jammed state is a first order phase transition: the final cluster concentrations C_k undergo a discontinuous jump so that $C_k(\lambda_c + 0) \neq C_k(\lambda_c)$ for $k = 1,2,\ldots$. The first order character of the phase transition is particularly evident in the case of monomers: their density vanishes for $\lambda \leqslant \lambda_c$ and remains positive in the supercritical region $\lambda > \lambda_c$.

A peculiar feature of our system is the dependence on the initial conditions. For the case of constant kernels, this dependence is simple: only the initial monomer density $c_{1,0}$ and the total density N_0 are important. For each value of $\lambda > 0$ there exists a domain in the phase plane $(N_0, c_{1,0})$ that corresponds to the supercritical regime where the system evolves to the universal equilibrium state. For the initial conditions outside this domain the system evolution terminates at jammed states. The size of this domain increases with the increasing λ. For $s > 0$, there still exists a domain in the space of initial conditions $\{c_1(0), c_2(0), \ldots, c_k(0), \ldots\}$, corresponding to the supercritical behavior. The location of this domain, however, is determined by all initial densities $c_k(0)$.

In spite of the simplicity of the model, it reflects some prominent features of the processes of the surface films growth. Hence, the possibility of the phase transition in such systems, as well as their dependence on the initial conditions, may be employed for practical manipulations of the surface films properties. It would be also interesting to study similar models in the context of self-assembly, perhaps generalizing the model to allow a few different types of monomers.

[1] M. V. Smoluchowski, Phys. Z. **17**, 557 (1916).

[2] P. L. Krapivsky, S. Redner, and E. Ben-Naim, *A Kinetic View of Statistical Physics* (Cambridge University Press, Cambridge, 2010).

[3] F. Leyvraz, Phys. Rep. **383**, 95 (2003).

[4] N. V. Brilliantov and P. L. Krapivsky, J. Phys. A: Math. Gen. **24**, 4789 (1991).

[5] J. A. Blackman and A. Wielding, Eorophys. Lett. **16**, 115 (1991).

[6] J. A. Blackman and A. Marshall, J. Phys. A: Math. Gen. **27**, 725 (1994).

[7] V. Privman, D. V. Goia, J. Park, and E. Matijevic, J. Colloid Interface Sci. **213**, 36 (1999).

[8] P. Laurençot, Nonlinearity **12**, 229 (1999).

[9] V. Gorshkov and V. Privman, Phys. E (Amsterdam) **43**, 1 (2010).

[10] I. Sevonkaev, V. Privman, and D. Goia, J. Chem. Phys. **138**, 014703 (2013).

[11] T. Poeschel, N. V. Brilliantov, and C. Frommel, Biophys. J. **85**, 3460 (2003).

[12] P. W. K. Rothemund, N. Papadakis, and E. Winfree, PLoS Biol. **2**, e424 (2004).

[13] K. Ariga, J. P. Hill, M. V. Lee, A. Vinu, R. Charvet, and S. Acharya, Sci. Tech. Adv. Mater. **9**, 014109 (2008).

[14] V. Privman, Ann. N. Y. Acad. Sci. **1161**, 508 (2009).

[15] A. Demortière, A. Snezhko, M. V. Sapozhnikov, N. Becker, T. Proslier, and I. S. Aranson, Nature Commun. **5**, 3117 (2014).

[16] C. G. Evans and E. Winfree, Chem. Soc. Rev. **46**, 3808 (2017).

[17] M. C. Bartelt and J. W. Evans, Phys. Rev. B **46**, 12675 (1992).

[18] H. Kallabis, P. L. Krapivsky, and D. E. Wolf, Eur. Phys. J. B **5**, 801 (1998).

[19] A. Pimpinelli and J. Villain, *Physics of Crystal Growth* (Cambridge University Press, Cambridge, 1998).

[20] M. Zinke-Allmang, Thin Solid Films **346**, 1 (1999).

[21] P. L. Krapivsky, J. F. F. Mendes, and S. Redner, Eur. Phys. J. B **4**, 401 (1998).

[22] P. L. Krapivsky, J. F. F. Mendes, and S. Redner, Phys. Rev. B **59**, 15950 (1999).
[23] J. G. Amar, M. N. Popescu, and F. Family, Phys. Rev. Lett. **86**, 3092 (2001).
[24] M. N. Popescu, J. G. Amar, and F. Family, Phys. Rev. B **64**, 205404 (2001).
[25] J. A. Blackman, Phys. A (Amsterdam) **220**, 85 (1995).
[26] J. A. D. Wattis, Phys. D (Amsterdam) **222**, 1 (2006).
[27] Y. Han, M. Li, and J. W. Evans, J. Chem. Phys. **145**, 211911 (2016).
[28] N. V. Brilliantov, P. L. Krapivsky, A. Bodrova, F. Spahn, H. Hayakawa, V. Stadnichuk, and J. Schmidt, Proc. Natl. Acad. Sci. USA **112**, 9536 (2015).
[29] S. A. Matveev, P. L. Krapivsky, A. P. Smirnov, E. E. Tyrtyshnikov, and N. V. Brilliantov, arXiv:1708.01604.